

Deposition of a Mo doped GaN thin film on glass substrate by thermionic vacuum arc (TVA)

Soner Özen¹ · Volkan Şenay^{1,2} · Suat Pat¹ · Şadan Korkmaz¹

Received: 6 January 2015 / Accepted: 31 March 2015 / Published online: 4 April 2015
© Springer Science+Business Media New York 2015

Abstract Current research presents a new deposition method for GaN thin films that produces in a very short production time for GaN-based solid-state applications. A Mo doped GaN thin film on a glass substrate was produced by thermionic vacuum arc (TVA) technique. The TVA technique is a novel non-reactive plasma technique. The optical properties were determined by Filmetrics F20 interferometer and UV–Vis double beam spectrophotometer. The surface morphology was analyzed using field emission scanning electron microscopy and atomic force microscopy. The mean thickness value was measured as 100 nm by Filmetrics interferometer. The crystalline structure of the produced thin film has a Wurtzite crystal structure (004) as obtained by X-ray diffraction. Hardness value was determined as 14 GPa with the Oliver–Pharr method. The obtained properties are consistent with the values reported in related literature. The findings indicate that the TVA method provides advantages for optical and industrial applications.

1 Introduction

GaN is a direct wide-bandgap semiconductor with good thermal conductivity and notable optical, mechanical, piezoelectric, and transport properties. It is widely used in

electrically pumped ultraviolet–blue light-emitting diodes, lasers, tunable mechanical resonators and switches, among other possible new sensor and transducer technologies as well as high power and high frequency applications [1–4]. GaN thin films have been deposited on various substrates such as Al₂O₃, SiC, GaAs, etc [4–8]. Gautier et al. [8] claimed that direct growth of III-nitride photovoltaics were not possible onto a glass. We have managed to perform the GaN thin film production onto glass. GaN films have approximately a band gap of 3.4 eV at 300 K [9–12], hardness value in the range of 4–18 GPa and Young’s modulus value in the range of 210–295 GPa [2, 10]. GaN films undergo a change in physical properties by doping [3, 9, 13–16]. Gallium nitride (GaN) growth techniques have been extensively studied for the past two decades. Growth techniques of GaN and doped GaN can be given as thermal decomposition [1, 5, 9], metal organic chemical vapor deposition (MOCVD) [4, 8, 13–15], magnetron sputtering [11], sol–gel process [17, 18], molecular beam epitaxy (MBE) [19], spin coating [20].

In this study, a Mo doped GaN thin film was produced using a non-reactive thermionic vacuum arc (TVA) method for the first time. TVA method can be used to produce thin films of various materials like metals, alloys, ceramics, silver diamond like carbon and refractory metals such as W, Mo, Ta, Nb, Re and B. TVA technique has a number of significant advantages for thin film growth. These advantages include being homogenous, compact and nano-structured, along with having a low roughness, good adhesion, a high deposition rate and a very short production time [21–30]. This research presents a new deposition mechanism for GaN-based solid-state applications. Doping process of GaN in TVA system is very simple according to other metal organic deposition process.

✉ Soner Özen
osoner@ogu.edu.tr

¹ Physics Department, Eskişehir Osmangazi University, 26480 Eskişehir, Turkey

² Primary Science Education Department, Bayburt University, 69000 Bayburt, Turkey

2 Experimental

TVA ignites in high or ultra-high vacuum condition between a heated cathode and an anode containing the material to be deposited without using any buffer gas. The accelerated electrons with high dc voltage collide with the anode. Due to the electron bombardment of the anode by the accelerated thermo-electrons from the cathode, the anode material starts to melt first. Subsequently, the anode material evaporates and a steady state concentration of the evaporated atoms of anode materials is ensured between the anode and the cathode. By increasing high voltage applied between the anode and the cathode space, a bright discharge is established in the vapors of the anode material in the vacuum chamber. The vapors of the anode material spread toward the wall of the vacuum chamber. Thus, top surface of the glass substrate was coated with anode material(s); source material(s). A glass substrate was located at a distance of 70 mm above the anode. The temperature of the glass substrate in the film deposition process is a little higher than the room temperature; approximately 40–50 °C. 0.3 g of GaN (MTI Corporation, c-axis SP1) crystal and 0.02 g of Mo (Alfa Aesar, 99.7 %) pellets were used as the anode material in a tungsten crucible. The working parameters of the TVA are summarized in Table 1.

Rigaku-rint-2200 X-ray diffraction (XRD) analysis was performed in the 2θ range of 40°–80° to investigate the crystalline structure of the produced thin film. Zeiss Supra 40VP field emission scanning electron microscopy (FESEM) and Ambios Q-Scope AFM (AFM) devices were used for the surface morphology characterizations of the Mo doped GaN film coated glass. AFM device was used for the investigation of the roughness and the nano-indentation. The AFM images were collected in non-contact imaging mode in ambient atmosphere. Energy dispersive X-ray spectroscopy was also used for the surface composition and elemental analyses. The transmittance and absorbance of the produced film was determined in the wavelength range of 200–1100 nm using an UNICO 4802 UV–Vis double beam spectrophotometer. The thickness,

Table 1 TVA working parameters for Mo doped GaN thin film on glass substrate

| Working parameters | Unit | Value |
|--------------------|------|--------------------|
| Working pressure | Torr | 4×10^{-5} |
| Voltage | V | 900 |
| Filament current | A | 18 |
| Discharge current | A | 0.8 |
| Deposition time | s | 60 |
| Deposition rate | nm/s | 1.7 |

reflection and spectral refractive index were measured using a Filmetrics F20 thin film analyzer which is an optical nondestructive system.

3 Result and discussion

An X-ray diffractometer with $\text{Cu-K}\alpha_1$ radiation ($\lambda = 1.5406 \text{ \AA}$) as the radiation source was used to analyze the crystallographic structures of the produced film. The X-ray diffraction patterns of the produced film seen in Fig. 1 exhibited diffraction peaks at 45.4° and 72.9°, corresponding to the (110) peak of the Ga structure (reference data code: 98-001-2174) and the (004) peak of the Wurtzite GaN crystal structure [5, 9, 20] as reported in existing literature, respectively. The EDX results of Mo doped GaN coated thin film is presented in Table 2. Its doping ratio was estimated through EDX measurement to be approximately 7 % Mo.

The surface characteristics were calculated by the ScanAtomic SPM software-2009 (Q-Port version 5.1.0). According to the AFM analysis, the surface roughness, average height, root-mean-square (RMS) deviation and mean deviation are 5, 10, 9 and 4 nm, respectively. The topography of the film surface in 2D image (Fig. 2a), 3D image (Fig. 2b) and FESEM image (Fig. 2c) are shown in Fig. 2. As seen in FESEM image, the Mo doped GaN film has a granular structure and the grain size is approximately 50 nm. The AFM images also support the FESEM image.

The optical properties of the produced thin film are shown in Fig. 3. The absorbance and transmittance spectra of the produced film were recorded by UV–Vis spectrometer between wavelengths of 200 and 1100 nm showed

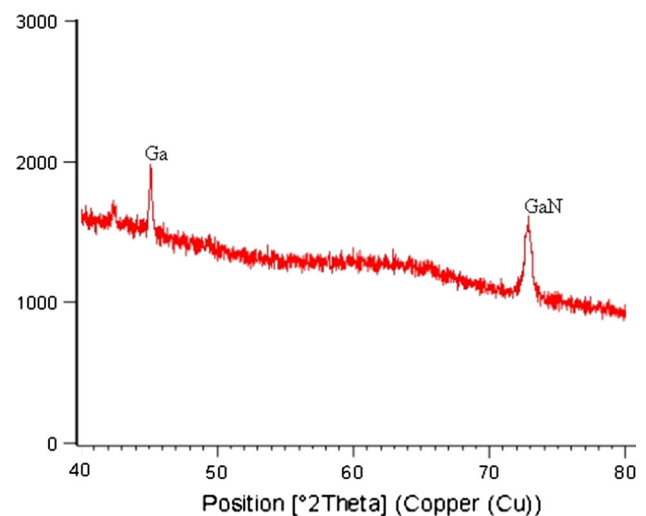


Fig. 1 X-ray-diffraction patterns of the 7 % Mo doped GaN thin film

Table 2 EDX result of the Mo doped GaN/glass thin film

| Element | Weight (wt%) | Atomic (at.%) |
|------------|--------------|---------------|
| Nitrogen | 14.2 | 46.3 |
| Gallium | 71.9 | 47.1 |
| Molybdenum | 13.9 | 6.6 |
| Toplam | 100.00 | 100.00 |

in Fig. 2a. As is observed, the Mo doped GaN thin film is highly absorbent in the wavelength range from 200 to 370 nm. The reflectance versus the wavelength between 400 and 1000 nm of produced thin film is presented Fig. 3b. In accordance with GaN reflectance characterization [31], the reflectance is approximately 30 % at 400 nm. Reflectance ratio is between 0 and 25 %. The refractive index determined by Filmetrics F20 is 2.22 at 550 nm and its change is 0.02 in the range of all measured wavelength.

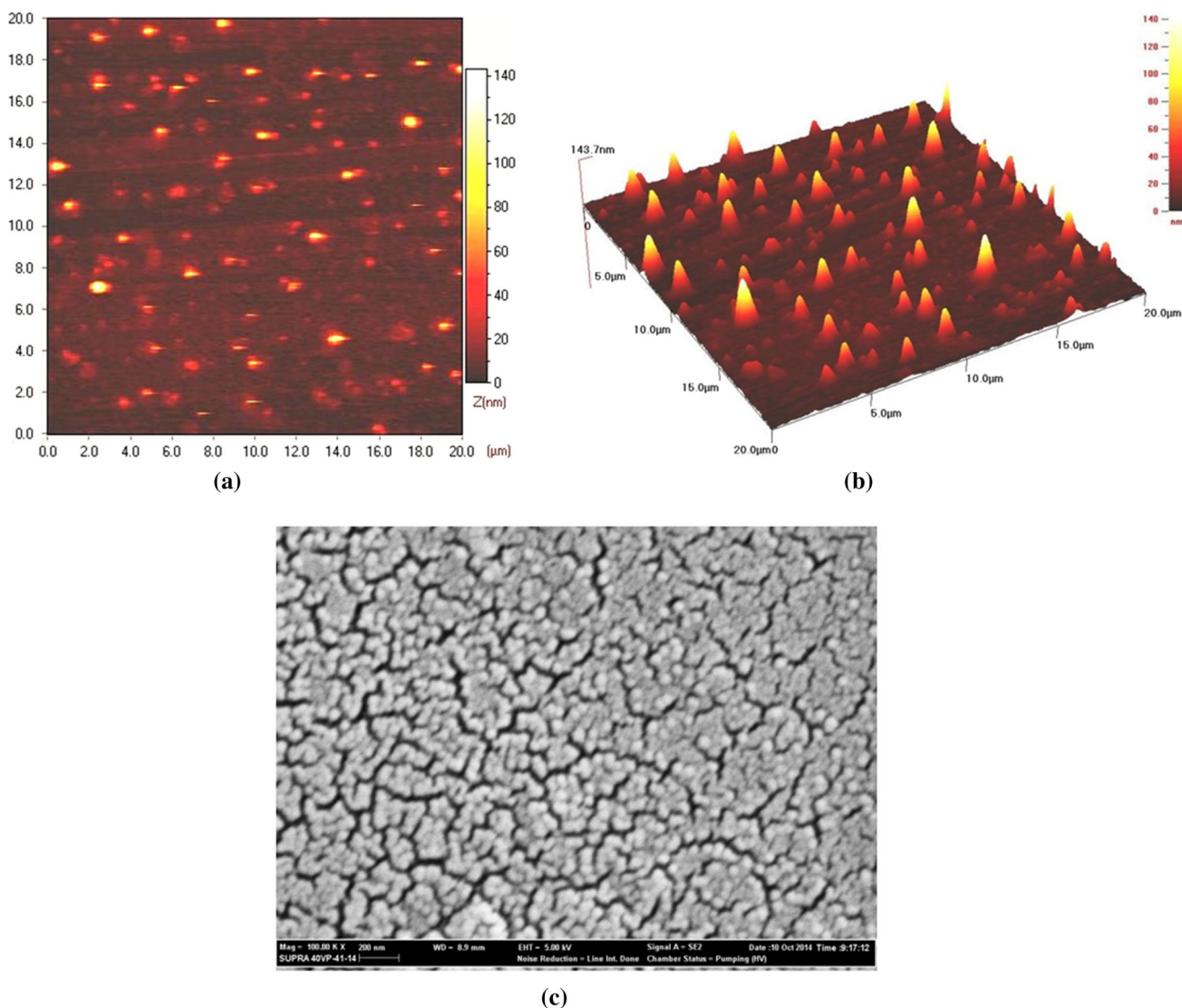
The optical band gap of the film is defined by using its absorbance data. Band gap of Mo doped GaN film was calculated using the expression

$$\alpha h\nu \approx (h\nu - E_g)^{1/2} \quad (1)$$

where $h\nu$ is the incident photon energy, E_g denotes the optical band gap and α is absorption coefficient [32]. The extrapolation of the linear part of the Tauc plot $(\alpha h\nu)^2$ versus $h\nu$ is plotted in Fig. 3d. Band gap energy was found to be around 3.3 eV.

AFM nano-indentation is a powerful technique for observing the nano-mechanical properties of the nano-structured materials. The Oliver–Pharr (O&P) method has been widely used for extracting the value of hardness from the nano-indentation data. According to the Oliver–Pharr approach, the hardness is given by [33, 34]

$$H = P_{\max}/A \quad (2)$$

**Fig. 2** a 2D-AFM image, b 3D-AFM image and c FESEM image of the Mo doped GaN thin film

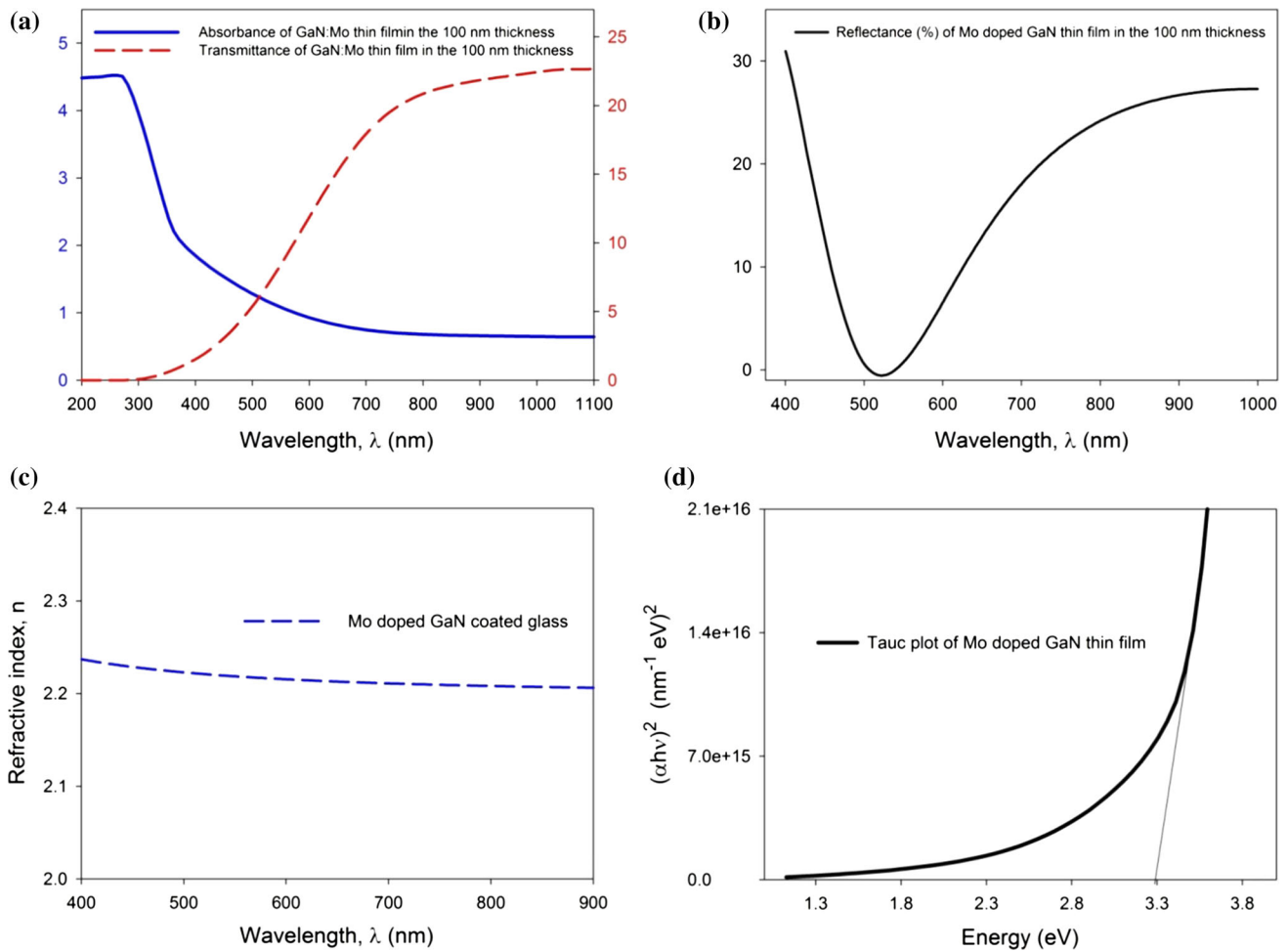


Fig. 3 **a** Absorbance and transmittance, **b** reflectance, **c** refractive index and **d** band gap energy graphs which optical properties of the Mo doped GaN thin film

where H is the hardness, P_{max} is the maximum applied load, and A is the projected contact area at the maximum applied load, which is determined by the geometry of the indenter and the contact depth, h_c . The area function for a perfect Berkovich indenter $A = 24.5 h_c^2$ can be used to provide a first estimate of the contact area. The hardness value of the produced thin film at 10 nm nano-indentation depth is calculated as 14 GPa. This hardness value is in good agreement with the relevant literature [2, 10]. Nano-indentation experiments should be realized at approximately 10–20 % of the film thickness [21, 35].

4 Conclusion

In this research, Mo doped GaN thin film on the glass substrate is deposited by the TVA technique. The deposition rate of the thin film on glass substrate was determined as 1.7 nm/s. The main advantage of this production technique is its high deposition rate without any loss in the

quality of the thin film. The material properties of the produced thin film are affected by the structure, surface states of substrate and Mo doping. XRD peak observed at 72.9° corresponds to the (004) orientation of Wurtzite GaN. The band gap energy value decreases with 7 % Mo doping. The decrease of the band gap energy by doping with transition metals is an expected result. Mo doped GaN is nanostructured with the hardness of 14 GPa and refractive index of 2.2. The results show that TVA is suitable for coating the glass substrate. TVA systems and working costs are very low compared to other metal organic vapor deposition systems. It can be concluded that TVA technique would be useful for industrial applications.

References

1. J.C. Johnson, H.J. Choi, K.P. Knutsen, R.D. Schaller, P. Yang, R.J. Saykally, Nat. Mater. **1**(2), 106–110 (2002). doi:[10.1038/nmat728](https://doi.org/10.1038/nmat728)

2. J.J. Brown, A.I. Baca, K.A. Bertness, D.A. Dikin, R.S. Ruoff, V.M. Bright, *Sens. Actuators A* **166**(2), 177–186 (2011). doi:[10.1016/j.sna.2010.04.002](https://doi.org/10.1016/j.sna.2010.04.002)
3. H. Morkoc, S. Strite, G.B. Gao, M.E. Lin, B. Sverdlov, M. Burns, *J. Appl. Phys.* **76**(3), 1363–1398 (1994). doi:[10.1063/1.358463](https://doi.org/10.1063/1.358463)
4. C. Sartel, S. Gautier, S. Ould Saad Hamady, N. Maloufi, J. Martin, A. Sirenko, A. Ougazzaden, *Superlattices Microstruct.* **40**(4), 476–482 (2006). doi:[10.1016/j.spmi.2006.09.026](https://doi.org/10.1016/j.spmi.2006.09.026)
5. J. Goldberger, R. He, Y. Zhang, S. Lee, H. Yan, H.J. Choi, P. Yang, *Nature* **422**(6932), 599–602 (2003). doi:[10.1038/nature01551](https://doi.org/10.1038/nature01551)
6. P. Waltereit, O. Brandt, A. Trampert, M. Ramsteiner, M. Reiche, M. Qi, K.H. Ploog, *Appl. Phys. Lett.* **74**(24), 3660–3662 (1999). doi:[10.1063/1.123214](https://doi.org/10.1063/1.123214)
7. A. Trampert, O. Brandt, H. Yang, K.H. Ploog, *Appl. Phys. Lett.* **70**(5), 583–585 (1997). doi:[10.1063/1.118281](https://doi.org/10.1063/1.118281)
8. S. Gautier, T. Moudakir, G. Patriarche, D.J. Rogers, V.E. Sandana, F. Hosseini Teherani et al., *J. Cryst. Growth* **370**, 63–67 (2013). doi:[10.1016/j.jcrysgro.2012.08.048](https://doi.org/10.1016/j.jcrysgro.2012.08.048)
9. S.E. Park, H.J. Lee, Y. Chan Cho, S.Y. Jeong, C. Ryong Cho, S. Cho, *Appl. Phys. Lett.* **80**(22), 4187–4189 (2002). doi:[10.1063/1.1483115](https://doi.org/10.1063/1.1483115)
10. H.Y. Huang, Z.Y. Li, J.Y. Lu, Z.J. Wang, C.S. Wang, K.M. Lau et al., *J. Micromech. Microeng.* **19**(9), 095019 (2009). doi:[10.1088/0960-1317/19/9/095019](https://doi.org/10.1088/0960-1317/19/9/095019)
11. D.W. Kang, J.Y. Kwon, J. Shim, H.M. Lee, M.K. Han, *Sol. Energy Mater. Sol. Cells* **105**, 317–321 (2012). doi:[10.1016/j.solmat.2012.06.041](https://doi.org/10.1016/j.solmat.2012.06.041)
12. S.L. Selvaraj, A. Watanabe, T. Egawa, *Appl. Phys. Lett.* **98**(25), 252105 (2011). doi:[10.1063/1.3602919](https://doi.org/10.1063/1.3602919)
13. A. Majid, A. Dar, A. Nabi, A. Shakoob, N. Hassan, A. Junjua, Z. Jianjun, *Mater. Chem. Phys.* **136**(2), 809–815 (2012). doi:[10.1016/j.matchemphys.2012.08.002](https://doi.org/10.1016/j.matchemphys.2012.08.002)
14. S. Heikman, S. Keller, S.P. DenBaars, U.K. Mishra, *Appl. Phys. Lett.* **81**(3), 439–441 (2002). doi:[10.1063/1.1490396](https://doi.org/10.1063/1.1490396)
15. A. Uedono, S. Ishibashi, K. Tenjinbayashi, T. Tsutsui, K. Nakahara, D. Takamizu, S.F. Chichibu, *J. Appl. Phys.* **111**(1), 014508 (2012). doi:[10.1063/1.3675516](https://doi.org/10.1063/1.3675516)
16. L. Zhang, K. Ding, N.X. Liu, T.B. Wei, X.L. Ji, P. Ma et al., *Appl. Phys. Lett.* **98**(10), 101110 (2011). doi:[10.1063/1.3565173](https://doi.org/10.1063/1.3565173)
17. G. Sinha, K. Adhikary, S. Chaudhuri, *Appl. Surf. Sci.* **254**(16), 5257–5260 (2008). doi:[10.1016/j.apsusc.2008.02.033](https://doi.org/10.1016/j.apsusc.2008.02.033)
18. H. Qiu, C. Cao, H. Zhu, *Mater. Sci. Eng. B* **136**(1), 33–36 (2007). doi:[10.1016/j.mseb.2006.08.026](https://doi.org/10.1016/j.mseb.2006.08.026)
19. M.J. Paisley, Z. Sitar, J.B. Posthill, R.F. Davis, *J. Vac. Sci. Technol. A* **7**(3), 701–705 (1989). doi:[10.1116/1.575869](https://doi.org/10.1116/1.575869)
20. M. Puchinger, T. Wagner, D. Rodewald, J. Bill, F. Aldinger, F.F. Lange, *J. Cryst. Growth* **208**(1), 153–159 (2000). doi:[10.1016/S0022-0248\(99\)00416-9](https://doi.org/10.1016/S0022-0248(99)00416-9)
21. S. Pat, M.Z. Balbağ, Ş. Korkmaz, *Ceram. Int.* **40**(7), 10159–10162 (2014). doi:[10.1016/j.ceramint.2014.02.041](https://doi.org/10.1016/j.ceramint.2014.02.041)
22. S. Pat, M. Özümücü, N. Ekem, M. Özkan, Ş. Korkmaz, M.Z. Balbağ, *J. Plast. Film Sheeting* **26**(3), 259–270 (2010). doi:[10.1177/8756087910392082](https://doi.org/10.1177/8756087910392082)
23. S. Pat, S. Temel, N. Ekem, Ş. Korkmaz, M. Özkan, M.Z. Balbağ, *J. Plast. Film Sheeting* **27**(1–2), 127–137 (2011). doi:[10.1177/8756087911399893](https://doi.org/10.1177/8756087911399893)
24. S. Pat, M.Z. Balbağ, Ş. Korkmaz, *NANO* (2013). doi:[10.1142/S1793292013500288](https://doi.org/10.1142/S1793292013500288)
25. N.E. Çetin, Ş. Korkmaz, S. Elmas, N. Ekem, S. Pat, M.Z. Balbağ et al., *Mater. Lett.* **91**, 175–178 (2013). doi:[10.1016/j.matlet.2012.07.086](https://doi.org/10.1016/j.matlet.2012.07.086)
26. H. Ehrich, J. Schuhmann, G. Musa, A. Popescu, I. Mustata, *Thin Solid Films* **333**(1), 95–102 (1998). doi:[10.1016/S0040-6090\(98\)00842-6](https://doi.org/10.1016/S0040-6090(98)00842-6)
27. C.P. Lungu, I. Mustata, G. Musa, V. Zaroschi, A. Mihaela Lungu, K. Iwasaki, *Vacuum* **76**(2), 127–130 (2004). doi:[10.1016/j.vacuum.2004.07.002](https://doi.org/10.1016/j.vacuum.2004.07.002)
28. C. Biloiu, H. Ehrich, G. Musa, *J. Vac. Sci. Technol. A* **19**(3), 757–761 (2001). doi:[10.1116/1.1368839](https://doi.org/10.1116/1.1368839)
29. M.Z. Balbag, S. Pat, M. Ozkan, N. Ekem, G. Musa, *Phys. B* **405**(16), 3276–3278 (2010). doi:[10.1016/j.physb.2010.04.059](https://doi.org/10.1016/j.physb.2010.04.059)
30. S. Pat, Ş. Korkmaz, S. Özen, V. Şenay, *J. Mater. Sci. Mater. Electron.* **26**(4), 2210–2214 (2015). doi:[10.1007/s10854-015-2670-7](https://doi.org/10.1007/s10854-015-2670-7)
31. K. Kornitzer, T. Ebner, M. Grehl, K. Thonke, R. Sauer, C. Kirchner et al., *Phys. Status Solidi B* **216**(1), 5–9 (1999). doi:[10.1002/\(SICI\)1521-3951\(199911\)216:1<5:AID-PSSB5>3.0.CO;2-F](https://doi.org/10.1002/(SICI)1521-3951(199911)216:1<5:AID-PSSB5>3.0.CO;2-F)
32. V. Şenay, S. Pat, Ş. Korkmaz, T. Aydoğmuş, S. Elmas, S. Özen et al., *Appl. Surf. Sci.* **318**, 2–5 (2014). doi:[10.1016/j.apsusc.2013.10.044](https://doi.org/10.1016/j.apsusc.2013.10.044)
33. W.C. Oliver, G.M. Pharr, *J. Mater. Res.* **7**(06), 1564–1583 (1992). doi:[10.1557/JMR.1992.1564](https://doi.org/10.1557/JMR.1992.1564)
34. W.C. Oliver, G.M. Pharr, *J. Mater. Res.* **19**(01), 3–20 (2004). doi:[10.1557/jmr.2004.19.1.3](https://doi.org/10.1557/jmr.2004.19.1.3)
35. L.A. Dunyushkina, E.O. Smirnova, S.V. Smirnov, V.M. Kuimov, S.V. Plaksin, *Ionics* **19**(3), 511–515 (2013). doi:[10.1007/s11581-012-0769-x](https://doi.org/10.1007/s11581-012-0769-x)